A Hierarchical Optimization Method for Deformation Force Monitoring Layout of Annular Parts

DAI Kaining[1], *LIU Changqing*[1], *WANG Enning*[1], *ZHAO Zhiwei*[1], *SALONITIS Konstantino*[2], *LI Yingguang*[1*]

1. College of Mechanical & Electrical Engineering, Nanjing University of Aeronautics and Astronautics, Nanjing 210016, P. R. China;

2. Sustainable Manufacturing Systems Centre, Cranfield University, Cranfield MK43 0AL, United Kingdom

(Received 31 March 2025; revised 14 June 2025; accepted 25 June 2025)

Abstract: Obtaining residual stress is crucial for controlling the machining deformation in annular parts, and can directly influence the performance and stability of key components in advanced equipment. Since existing research has achieved global residual stress field inference for components by using the deformation force-based method where the deformation force is monitored during the machining process, reliable acquisition of deformation force still remains a significant challenge under complex machining conditions. This paper proposes a hierarchical optimization method for the layout of deformation force monitoring of annular parts. The proposed method establishes two optimization objectives by analyzing the relationship between the deformation force and the residual stress in annular parts, i.e., equivalence and ill-conditioning of solving process. Specifically, the equivalence of the monitored deformation force and residual stress in terms of effect on caused machining deformation is evaluated by local deformation, and the ill-conditioning is also optimized to enhance the stability of residual stress inference. Verification is implemented in both simulation and actual machining experiments, demonstrating effectiveness of the proposed layout optimization method in inferring residual stress field of annular parts with deformation force.

Key words: residual stress; annular part; deformation force; layout optimization

CLC number: V262.3 **Document code:** A **Article ID:** 1005-1120(2025)03-0275-12

0 Introduction

Annular parts are widely used in power systems and load-bearing structures across advanced equipment manufacturing industries, with typical applications including aircraft engine casings, rocket shells and fuel tanks, and gas turbine casings[1-3]. The increasing demands for performance, precision, and reliability in advanced equipment have placed increasing stringent requirements on controlling machining-induced deformation.

Residual stress is widely acknowledged as a key contributor to machining deformation[4-5]. In particular, the high level of initial residual stress generated during the heat treatment and forming process of annular part blanks has been identified as a primary cause of this deformation[6-8]. Therefore, accurately obtaining the residual stress field is crucial for optimizing deformation control strategies[9-10]. However, direct measurement of the residual stress field in parts remains a significant challenge[11-12].

Methods inferring residual stress can be broadly classified into local inference methods and global-field inference methods. Recent research has demonstrated significant progress in local inference methods through data-driven methods. These methods focus on predicting characteristic stress quantities such as layer-wise stress and overall stress levels.

*Corresponding author, E-mail address: liyingguang@nuaa.edu.cn.

How to cite this article: DAI Kaining, LIU Changqing, WANG Enning, et al. A hierarchical optimization method for deformation force monitoring layout of annular parts[J]. Transactions of Nanjing University of Aeronautics and Astronautics, 2025, 42(3):275-286.

http://dx.doi.org/10.16356/j.1005-1120.2025.03.001

Khoshaim et al.[13] developed a hybrid AI model combining artificial neural networks (ANNs) with metaheuristic optimization to predict radial and circumferential overall residual stresses in dry turning of DT4E pure iron. Wang et al.[14] proposed a neural network-based stress generator method for inferring the initial residual stress in layers by fusing online monitoring data with a finite element simulation model. Cheng et al.[15] introduced a Gaussian process regression based model to robustly predict machining-induced surface residual stress, and optimized selection of features extracted from sensor data for prediction via the random forest method. Zhou et al.[16] developed an empirical, data-driven model using exponential decay cosine (EDC) functions optimized by the firefly algorithm and mapped via the support vector machine to predict overall residual stress level in multi-axis milling of GH4169G superalloy. Rissaki et al.[17] developed an ANN model to predict the axial and hoop residual stress along the thickness in girth-welded austenitic stainless-steel the pipes, achieving predictions that closely align with experimental data. Miao et al.[18] developed an ANN-based surrogate model of the finite element method (FEM) for predicting longitudinal post-weld residual stress profiles without relying on extensive experimental datasets. Farias et al.[19] proposed a hybrid machine learning approach that integrates principal component analysis for dimensionality reduction with a radial basis function network to predict overall machining-induced residual stress. Li et al.[20] trained and compared different machine learning models to predict the residual stress along depth in laser shock peening induced LD-TC4 alloy with FEM data. Pradhan et al.[21] proposed a Bayesian regularized neural network model to predict the maximum residual stress in ultrasonic surface rolling of lightweight alloys. However, these methods are generally limited in inferring the global-field of residual stress distribution, facing challenges in precise deformation control with obtained local residual stress.

In contrast, progress has been made in inferring the global distribution of residual stress, enabling a more comprehensive description of residual stress across entire parts. Zhao et al.[22] introduced the concept of deformation force and established its physical relationship with the global residual stress field, enabling the inference of residual stress field based on deformation force monitored during machining process. Compared with residual stress measurement techniques, the deformation force method is capable of inferring the global residual stress field of parts. This approach involves solving a volume coefficient matrix which is influenced by the deformation force monitoring layout, thereby affecting the inference accuracy. To achieve accurate residual stress field inference in annular parts with deformation force, it is necessary to optimize the deformation force monitoring layout for annular parts.

In the context of deformation force monitoring layout for annular parts, increasing the number of monitoring points can provide richer monitoring information. However, the geometric constraints and machining requirements of annular parts limit the number and placement of feasible monitoring points. As a result, the equivalence between the monitored deformation force and the residual stress field is further influenced. Moreover, since the monitored deformation force represents a lower-dimensional observation compared to the residual stress field to be inferred, the inference becomes a severely underdetermined inverse problem. This leads to ill-conditioning of the system matrix during the solution process. The causes and consequences of such ill-conditioning have been extensively investigated in literature. Algredo-Badillo et al.[23] investigated ill-conditioning in problem-solving using matrix representations. Through practical case studies, they analyzed the substantial impact of errors in unstable systems with ill-conditioning and examined how accuracy and ill-conditioning influence the system. Gui et al.[24] analyzed the relationship between the two primary methods used in ill-conditioning analysis, i.e. the eigenvalue analysis method and the condition number method, comparing their respective advantages and limitations. Li et al.[25] explored the accuracy and stability of solving linear equations using truncated singular value decomposition and Tikhonov regulariza-

tion, deriving bounds for the effective condition number to mitigate ill-conditioning in these methods. Reichel et al.[26] investigated the influence of the regularization parameter on solution quality in regularized approaches to ill-conditioned problems and evaluated the performance of different parameter selection strategies. Dewaele et al.[27] proposed a latent condition number framework based on feasible constant-rank equations to identify the constraints causing ill-conditioning within a numerical problem by analyzing the effect of constraint relaxation.

Therefore, since the accuracy of inferring the residual stress field in an annular part critically depends on the arrangement of deformation force sensors, it is essential to establish a systematic method for designing an optimal monitoring layout. To this end, the deformation force monitoring layout for the annular part is formulated as a multi-objective optimization problem with the following two objectives: (1) Enhancing the equivalence between the effects of the measured deformation force and the residual stress field on machining deformation; (2) reducing the ill-conditioning of the volume coefficient matrix.

To address these challenges, a hierarchical optimization method for deformation force monitoring layout of annular parts is proposed in this paper. The optimization objectives are derived from accuracy of residual stress inference, based on the thick-walled cylinder theory. A genetic algorithm (GA) is employed to minimize the local deformation under varying numbers of monitoring points. Additionally, the condition number of the volume coefficient matrix is introduced as a second objective to assess ill-conditioning. This approach ensures both the equivalence between the influence of the deformation force and the residual stress field on deformation, and the numerical stability of the inference process. The framework of the proposed optimization method for the deformation force monitoring layout of annular parts is illustrated in Fig.1.

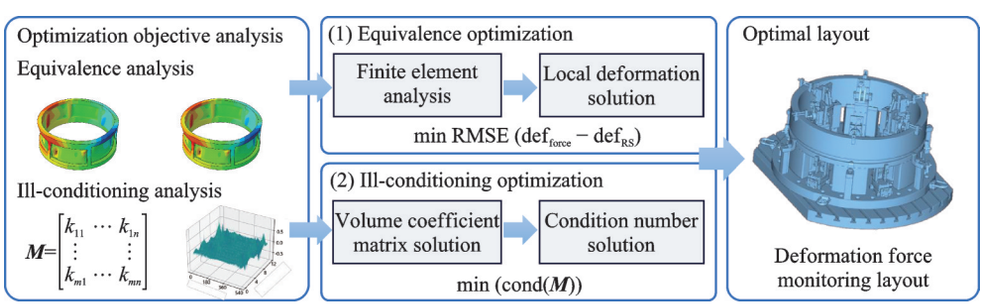

Fig.1 Framework of the deformation force monitoring point layout optimization method

1 Problem Analysis and Optimization

The deformation force monitoring layout of annular parts is a multi-objective optimization problem. The first objective is to enhance the equivalence between effects of the monitored deformation force and residual stress field on machining deformation. The second objective is to reduce the ill-conditioning in the inverse problem of the deformation force method. This section introduces the inference process of the residual stress field using the deformation force. To analyze and quantify both optimization objectives, the deformation behavior of annular parts is assessed based on the stress-deformation relationship described by a thick-walled cylinder model. In addition, the ill-conditioning of the volume coefficient matrix is analyzed. Through the analysis, the two objectives are quantified to guide the optimization of the deformation force monitoring layout.

1.1 Theory of residual stress field inference with deformation force

Before machining, the residual stress field within the part is in a state of equilibrium. As the material is removed during machining, the equilibrium is disrupted, causing reaction forces on the clamping regions. Upon release of the clamping device, the unbalanced residual stress field is redistributed to establish a new equilibrium, thereby induc-

ing machining deformation in the part. These forces exerted on the clamping device are referred to as deformation forces, whose effects on deformation are equivalent to the effects of the residual stress.

According to the description of the deformation force method in Ref.[22], the relationship between the deformation force $\boldsymbol{F}$ and the residual stress field $\boldsymbol{\sigma}_0$ can be expressed as

$$\boldsymbol{M}\boldsymbol{\sigma}_0 = \boldsymbol{F} \tag{1}$$

where $\boldsymbol{M}$ denotes the volume coefficient matrix. $\boldsymbol{M}$ is composed of elements M_{ij} representing the ratio of the deformation force to the residual stress in corresponding finite element cell. $\boldsymbol{M}$ is calculated through FEM since the finite element simulation has emerged as an effective and efficient approach for elucidating the physical mechanisms of cutting process[28].

Based on Eq.(1), the residual stress field can be inferred from the measured deformation forces acting on the annular part. However, achieving accurate inference requires both the precise deformation force and the low ill-conditioning of $\boldsymbol{M}$. The accuracy of the monitored deformation force is represented with local deformation, which is affected by the clamping layout. Meanwhile the calculation of $\boldsymbol{M}$ is related to the constrained condition of parts, i.e., clamping layouts. Therefore, it is necessary to optimize the clamping layout to improve the inference accuracy of the residual stress field.

1.2 Equivalence analysis of monitored deformation force

In order to analyze the equivalence of the deformation force, a mechanical model of the annular part is first established. Since the outer-to-inner radius ratio of the annular part used in this paper exceeds 1.1, the mechanical model of part is approximated by a thick-walled cylinder model[29]. Moreover, the geometry and load distribution of the model are symmetric with respect to the central axis, and no deformation occurs in the axial direction. Thereby, the model is simplified to a plane axisymmetric formulation for mechanistic analysis.

Based on the geometrical characteristic and machining conditions of the annular part, the following assumptions are made. The annular part contains a high level of initial residual stress. During the machining process, appropriate cutting parameters and cooling conditions are assumed such that the stress induced by cutting heat and cutting force are negligible compared to the initial residual stress. Additionally, the material removal thickness is small relative to the axial length of the part. Therefore, the effect of material removal on axial deformation is neglected.

Unknown variables in the plane axisymmetric problem include radial stress σ_r, hoop stress σ_θ, radial strain ε_r, hoop strain ε_θ, and radial displacement u. Through the finite element analysis, these variables satisfy the equilibrium equations, geometric equations and constitutive equations, respectively.

$$\frac{\mathrm{d}\sigma_r}{\mathrm{d}r} + \frac{\sigma_r - \sigma_\theta}{r} = 0 \tag{2}$$

$$\begin{cases} \varepsilon_r = \dfrac{\mathrm{d}u}{\mathrm{d}r} \\ \varepsilon_\theta = \dfrac{u}{r} \end{cases} \tag{3}$$

$$\begin{cases} \varepsilon_r = \dfrac{1}{E}(\sigma_r - \mu\sigma_\theta) \\ \varepsilon_\theta = \dfrac{1}{E}(\sigma_\theta - \mu\sigma_r) \end{cases} \tag{4}$$

where r is the radius coordinate; μ the Poisson's ratio; and E the Young's modulus.

We set a thick-walled cylinder with an inner radius a and an outer radius b, which is machined from b to a radius R_0. Then the effect of the redistributed residual stress caused by the material removal can be equivalently represented by a uniformly distributed external load p acting on the outer surface of the remaining material, as depicted in Fig.2.

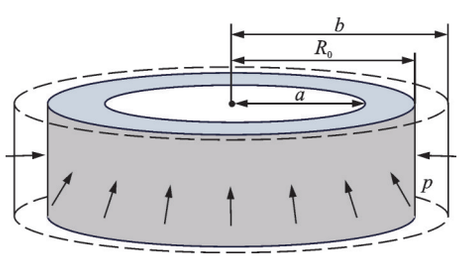

Fig.2 Mechanical analysis of thick-walled cylinder model

The boundary condition can be written as

$$\begin{cases} \sigma_r|_{r=a} = 0 \\ \sigma_r|_{r=R_0} = -p \end{cases} \tag{5}$$

By combining the boundary condition with the

three governing equations, the radial deformation induced by the redistributed residual stress can be expressed as Eq.(6). This equation characterizes the relationship between the equivalent external load and the resulting radial deformation of the annular part after the material removal.

$$u_r=\frac{1}{E}\left[-(1+\mu)\frac{a^2R_0^2p}{R_0^2-a^2}\frac{1}{r}+(\mu-1)\frac{R_0^2p}{R_0^2-a^2}r\right] \tag{6}$$

This analytical expression serves as the theoretical foundation for the residual stress inference model. It conceptually supports the assumption that the deformation induced by the residual stress can be equivalently represented by a set of deformation forces in annular parts. According to the analysis in Ref.[30] regarding the effect of the residual stress on deformation, the deflection change induced by the residual stress field can be equivalently represented by that caused by an infinitely dense distribution of concentrated forces. The principle guides the formulation of the optimization objective function, which seeks to maximize the equivalence between the deformation force and the residual stress field. However, in the practical machining environment, the sensor layout for annular parts is spatially constrained, allowing only a limited number of the deformation forces to be monitored.

Since the effect of outer loads other than deformation force is considered negligible, the difference between the deformation induced by the monitored deformation forces and the residual stress field is equivalent to the local deformation of the part. The local deformation is used as a metric to evaluate the equivalence between the deformation force and the residual stress field. This metric forms the first objective in the optimization of the deformation force monitoring layout, as represented

$$\min \mathrm{RMSE}(\mathrm{def}_{\mathrm{force}}-\mathrm{def}_{\mathrm{RS}}) \tag{7}$$

where $\mathrm{def}_{\mathrm{force}}$ is the deformation caused by deformation force; $\mathrm{def}_{\mathrm{RS}}$ the deformation caused by residual stress; and RMSE the root mean square error.

1.3 Ill-conditioning analysis of the residual stress field inference

In the mechanical relationship presented in Eq.(1) between the deformation force and the residual stress field, calculating $\boldsymbol{\sigma}_0$ requires inverting $\boldsymbol{M}$. However, $\boldsymbol{M}$ is an ill-conditioned matrix and calculated through FEM for specific sensor layout and part geometry. Ill-conditioning denotes a problem's sensitivity to small perturbation in the input, which can result in large errors in the solution. Consequently, it influences the stability of the solution process upon the presence of measurement noises in the deformation force.

The ill-conditioning of $\boldsymbol{M}$ originates from linear dependence among its column vectors. In the residual stress inference problem, poor sensor layouts can cause $\boldsymbol{F}$ to contain redundant strain observations from identical part regions. Since $\boldsymbol{M}$ is also derived based on specific sensor layout, linear dependence of eigenvectors in $\boldsymbol{M}$ is caused, leading to significant redundancy and ill-conditioning in $\boldsymbol{M}$. Such ill-conditioning amplifies the impact of even subtle errors in $\boldsymbol{F}$, causing considerable errors in the inferred residual stress field.

In Eq.(1), errors arising from the force sensor measurements lead to errors $\Delta\boldsymbol{F}$ in the measured deformation force. Consequently, it induces a reconstruction error $\Delta\boldsymbol{\sigma}$ in the inferred residual stress.

$$\boldsymbol{F}+\Delta\boldsymbol{F}=\boldsymbol{M}(\boldsymbol{\sigma}+\Delta\boldsymbol{\sigma}) \tag{8}$$

$$\Delta\boldsymbol{F}=\boldsymbol{M}\Delta\boldsymbol{\sigma} \tag{9}$$

The relative error can be presented as

$$\frac{\|\Delta\boldsymbol{\sigma}\|}{\|\boldsymbol{\sigma}\|}\leqslant\|\boldsymbol{M}^{-1}\|\|\boldsymbol{M}\|\frac{\|\Delta\boldsymbol{F}\|}{\|\boldsymbol{F}\|} \tag{10}$$

Ill-conditioning of $\boldsymbol{M}$ leads to redundancy and rank deficiency of matrix, thereby rendering the matrix nearly singular. Consequently, it amplifies errors, and compromises both the accuracy and stability of numerical computation. Thus, reducing ill-conditioning of $\boldsymbol{M}$ constitutes the second optimization objective.

The condition number $\mathrm{cond}(\boldsymbol{M})$ is a critical indicator of the ill-conditioning of $\boldsymbol{M}$, as presented

$$\mathrm{cond}(\boldsymbol{M})=\|\boldsymbol{M}^{-1}\|\|\boldsymbol{M}\| \tag{11}$$

A larger condition number indicates that disturbances in sensor signals have a greater impact on solution accuracy, rendering the matrix increasingly ill-conditioned. To evaluate the ill-conditioning of

$\boldsymbol{M}$, singular value decomposition (SVD) is performed.

$$\boldsymbol{M}_{m*n}=\boldsymbol{U}_{m*m}\boldsymbol{S}_{m*n}\boldsymbol{V}_{n*n}^{\mathrm{T}}=\sum_{i=1}^{n}\boldsymbol{u}_i\lambda_i\boldsymbol{v}_i^{\mathrm{T}} \tag{12}$$

where $\boldsymbol{U}$ and $\boldsymbol{V}$ are the left and the right singular matrices with column vectors $\boldsymbol{u}_i$ and $\boldsymbol{v}_i$, respectively; and $\boldsymbol{S}$ is a diagonal matrix composed of singular values λ_i, $\boldsymbol{S}=\mathrm{diag}(\lambda_1,\lambda_2,\cdots,\lambda_m)$ and $\lambda_1\geqslant\lambda_2\geqslant\cdots\geqslant\lambda_m$.

The condition number is calculated as the ratio of the largest singular value to the smallest singular value obtained from SVD

$$\mathrm{cond}(\boldsymbol{M})=\lambda_1/\lambda_m \tag{13}$$

Thus, the second objective to reduce ill-conditioning can be expressed with condition number as

$$\min\ \mathrm{cond}(\boldsymbol{M}) \tag{14}$$

2 Layout Optimization Method

For the deformation force monitoring of annular parts, the equivalence of the monitored deformation force directly affects the accuracy of the residual stress field inference, and ill-conditioning of $\boldsymbol{M}$ primarily influences the stability of the solution under measurement errors. Therefore, the overall optimization problem can be formulated as

$$\min_{x}\ \{\mathrm{RMSE}(\mathrm{def}_{\mathrm{force}}-\mathrm{def}_{\mathrm{RS}}),\ \mathrm{cond}(\boldsymbol{M})\}$$
$$x\in X_b \tag{15}$$

where x denotes the deformation force monitoring layout configuration; X_b the set of all monitoring layout configurations that satisfy the spatial constraints of annular parts machining and clamping stability.

However, computing entails a time-consuming process, as it involves both large-scale matrix inversion and finite element simulation. As a result, directly optimizing both objectives simultaneously would lead to a substantial computational burden and significantly prolong the optimization cycle.

To address this challenge and balance the trade-off between optimization efficiency and global search capability, this study proposes a hierarchical optimization strategy. By decomposing the multi-objective problem into prioritized levels, the proposed approach reduces the solution complexity while still guiding the search toward globally favorable solutions. The hierarchical structure of the optimization process is illustrated in Fig.3. Since local deformation directly represents the accuracy of the inferred residual stress field, maximizing the equivalence between the deformation force and the residual stress field is set as the primary optimization objective.

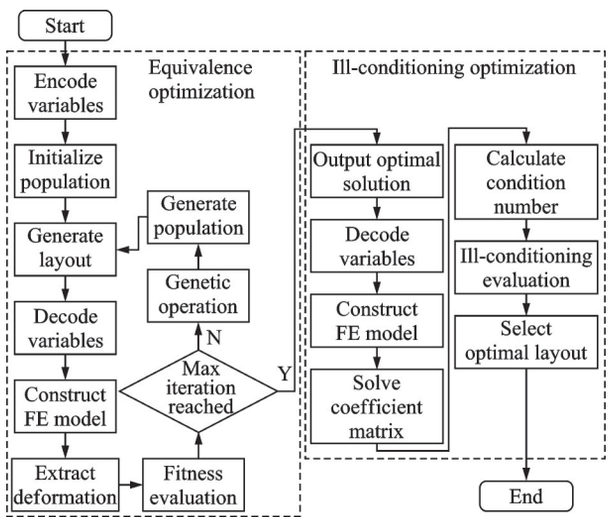

Fig.3 Process of the deformation force monitoring layout optimization for an annular part

Due to the global search capability and robustness in handling non-differential problems, GA is adopted to encode and optimize the sensor layout to achieve optimal equivalence between the deformation force and the residual stress field. Moreover, the discrete nature and computational efficiency of GA further enhance its adaptability compared with other optimization methods when interfacing with finite element simulations. A finite element model is constructed to decode and evaluate candidate layout schemes in each GA iteration. And ill-conditioning is subsequently incorporated to identify configurations with lower condition number.

In GA, variables are the locations of monitoring points, encoded as real numbers representing indices of the predefined candidate locations. These positions are selected based on the machining characteristics, clamping constraints, and axisymmetric characteristics of annular parts. Genetic operations are conducted with a roulette wheel selection strategy and a single-point crossover operator.

The fitness function in the GA is defined as the

reciprocal of the local deformation with an exponential scaling applied to amplify the impact.

$$\text{fitness} = e^{1/(\text{RMSE}(\text{def}_{\text{force}} - \text{def}_{\text{RS}}))} \tag{16}$$

Through GA, the optimal monitoring position layout are identified for different sensor numbers. Subsequently, each layout is further evaluated to minimize the ill-conditioning with the volume coefficient matrix $\boldsymbol{M}$ computed. The singular values are obtained via SVD and used to calculate the condition number as the ratio of the largest to the smallest singular value. The layout with the smallest condition number across different monitoring point numbers is finally selected as the optimal layout.

Thereby, the optimal number and positions of deformation force monitoring points can be efficiently determined, achieving maximized equivalence between the deformation force and the residual stress field while minimizing the ill-conditioning of the residual stress field inference.

3 Verification and Discussion

Based on the proposed hierarchical optimization method for the deformation force monitoring layout in annular parts, verification was conducted in both finite element simulation and real machining environment. Local deformation was used as the primary optimization objective in GA to generate layout configurations for different numbers of monitoring points. Subsequently, the optimal layout was selected based on the condition number of $\boldsymbol{M}$.

The annular part geometry used for verification is presented in Fig.4. The part features an inner diameter of 540 mm, an outer diameter of 600 mm, and a height of 140 mm. It is made of aluminum alloy 2A70, with a Young's modulus of 72 GPa and a Poisson's ratio of 0.33. The part was clamped by fixtures on the lower end face. Six material removal regions were evenly distributed along the circumference, with each operation removing a 2 mm thick layer. In total, 12 layers were removed with 72 individual material removal operations.

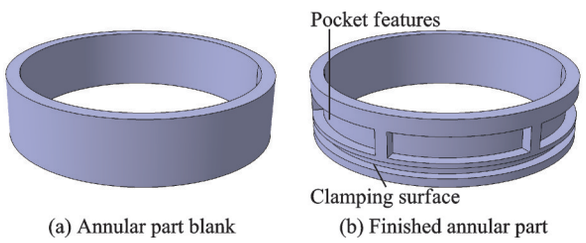

Fig.4 Geometric diagrams of the annular part

Considering the actual machining space constraints, 18 candidate positions on the inner surface were selected with 12 monitoring points located on the upper end surface and 6 at the lower end, as shown in Fig.5.

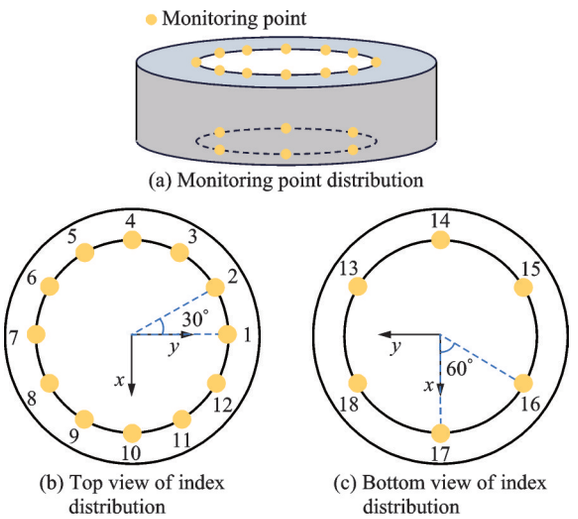

Fig.5 Distribution of monitoring points

3.1 Simulation verification

Simulation was conducted in Abaqus to model the annular part and simulate the material removal process. The positions of the monitoring points were adjusted based on the layout generated by GA. To represent the monitoring locations, variables were encoded as indices ranging from 1 to 18. GA was set with a population size of 40 and a maximum of 50 generations. Genetic operations included a roulette wheel selection strategy and a single-point crossover with a probability of 0.8. Additionally, the mutation operator randomly selected the gene of one monitoring point and replaced it with a new index with a probability of 0.02.

Derived from empirical measurements from prior experiments, approximate residual stress values were used as a predefined field. The deformation at the outer surface of the part was extracted to compute the fitness function in Eq.(12). Fig.6 illustrates the changes in the local deformation and fitness function values during the GA iteration.

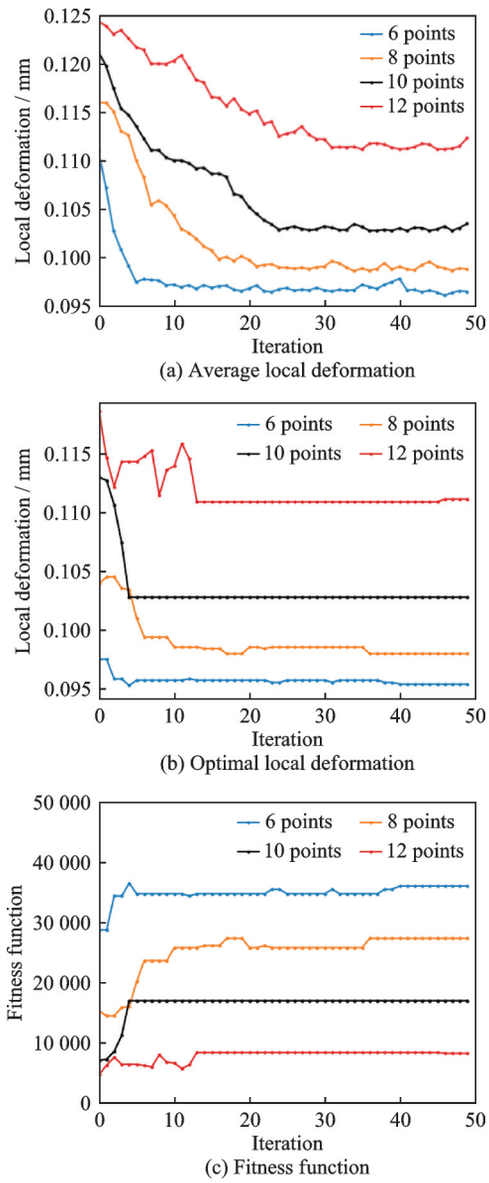

Fig.6 Convergence curves of GA

The iteration of the GA presents the optimization process of the local deformation embedded in the fitness function. It is indicated that the GA managed to maximize the equivalence between the effect of the deformation force and the residual force on deformation in the annular part. Optimal layout schemes were obtained for configurations with 6, 8, 10, and 12 monitoring points as displayed in Fig.7. The corresponding layout schemes are presented in Table 1.

The optimized results obtained from GA were compared with an evenly distributed layout scheme, commonly adopted as a default approach due to its simplicity and efficiency. For the deformation force monitoring layout of annular parts, the evenly distributed scheme placed an equal number of monitoring points at identical angles on the upper and lower ends of the part. The local deformation values of this scheme were 0.111, 0.115, 0.112, and 0.118 mm for configurations with 6, 8, 10, and 12 monitoring pointss respectively. In contrast, the local deformation of the result of the GA iteration demonstrates performance improvement, indicating that the GA achieves better equivalence between the residual stress and the deformation force.

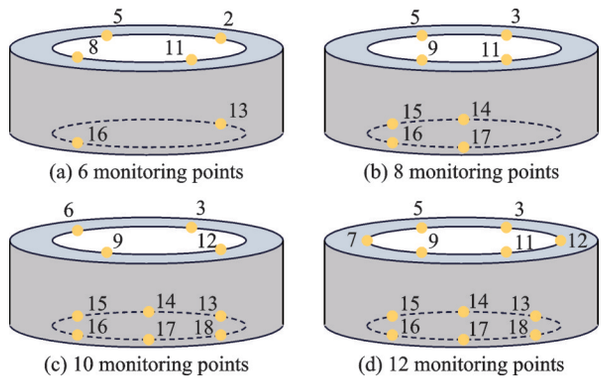

Fig.7 Distributions of optimized monitoring points by GA

Table 1 Optimization results of GA

Number of monitoring points	Index of monitoring points
6	[2,5,8,11,13,16]
8	[3,5,9,11,14—17]
10	[3,6,9,12—18]
12	[1,3,5,7,9,11,13—18]

Based on the optimal layout schemes with minimized local deformation for varying numbers of monitoring points, the corresponding volume coefficient matrix $\boldsymbol{M}$ was computed for each layout and subjected to SVD. The dimensions of $\boldsymbol{M}$ are 432×24, 576×24, 720×24, and 864×24 for different monitoring point numbers, with 24 singular values for each. The singular value distributions for each layout are depicted in Figs.8, 9.

Most of the singular value ratios were distributed within the range of 10 to 1 000, while a few fall below 10 or exceed 1 000. The condition numbers corresponding to each layout configurations are listed in Table 2. It can be inferred that the layout with 12 monitoring points exhibits the smallest condition number, which is selected as the final deformation force monitoring layout for the annular part.

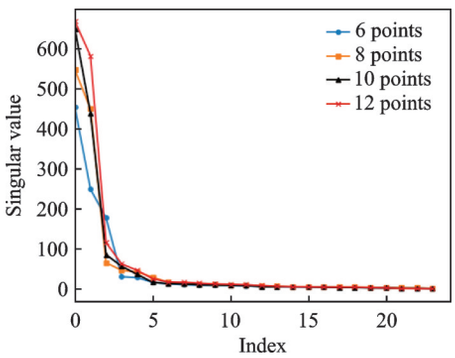

Fig.8 Distributions of singular values for different monitoring points

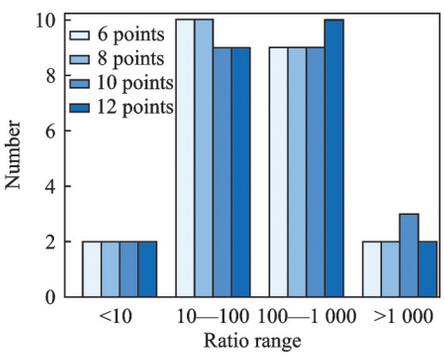

Fig.9 Distributions of singular value ratios for different monitoring points

Table 2 Condition number of layouts for different monitoring points

Monitoring point number	Condition number
6	2 571.653
8	2 217.833
10	2 626.223
12	2 136.197

3.2 Experimental verification

For the experimental validation, the annular part blank with the same dimensions described in the simulation setup was used as the workpiece. Machining validation was performed on a DMU 80P machining center, as shown in Fig.10. The machining parameters were set as follows: The spindle speed of 3 000 r/min, the feed rate of 2 000 mm/min, the cutting depth of 2 mm, and end mill diameter of 20 mm.

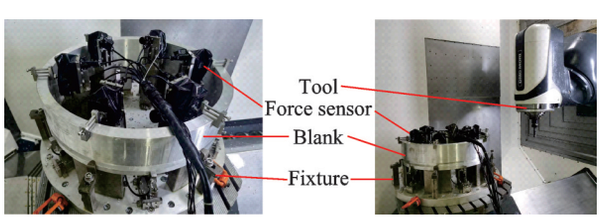

Fig.10 Experimental machining environment

Fixtures equipped with the deformation force sensors for annular parts were used to clamp the workpiece and measure the deformation force, as depicted in Fig.11. These fixtures provided fixed constraints and deformation force monitoring capabilities at the upper and the lower ends of the annular part.

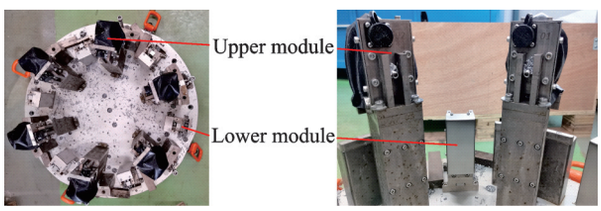

Fig.11 Experimental layout of deformation force monitoring

During the machining process, the material was removed by features and layers to obtain deformation forces. A total of 12 layers were removed, each 2 mm thick, with 6 features per layer. The monitoring points were arranged according to the results of hierarchical optimization. The strain signals recorded by the force sensors were converted into deformation force data using a multi-channel strain signal acquisition instrument.

After machining, the constraints at the deformation force monitoring points were removed to release and measure its deformation in the assembled state, while the clamping plate constraint was retained, as shown in Fig.12. The measurement points were located 5 mm below the top surface of the part and uniformly distributed along the circumference at 30° intervals, with a total of 12 measurement points.

Based on the deformation force monitoring data recorded during machining and computation of $\boldsymbol{M}$, the inferred residual stress fields are illustrated in Fig.13. The value of the residual stress ranges between −40 MPa and 40 MPa across most regions,

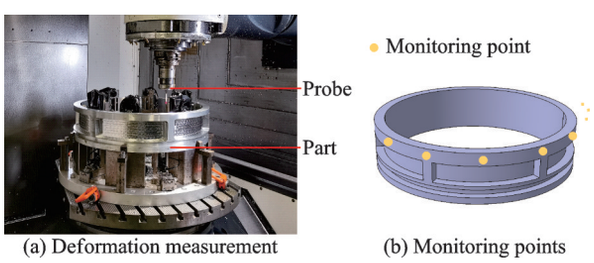

Fig.12 Measurement of machining deformation

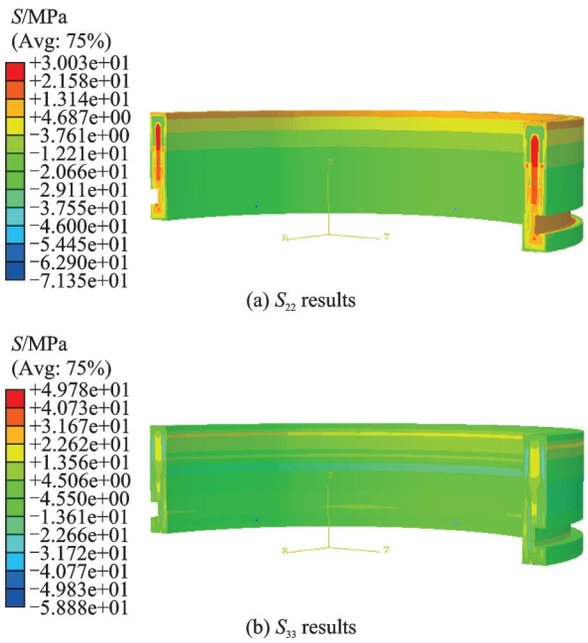

Fig.13 Inference results of residual stress field

with the tensile stress observed in the internal regions and compressive stress at the surface.

Since accurately measuring the global residual stress field in actual parts is challenging, validation of the inference was conducted through an estimation method in simulation. Specifically, the inferred residual stress field was applied to an identical part blank in simulation, followed by simulated material removal process. Subsequently, the resulting deformation and deformation force from the simulation were compared with the experimental measurements.

The result of deformation comparison between measurement and simulation based on the inferred residual stress is presented in Fig.14. It shows that the average absolute error in the predicted deformation is 0.037 mm, with a maximum absolute error of 0.105 mm. Meanwhile, the average absolute error in the predicted deformation force is 20.858 N, with a maximum error of 70.736 N. The difference of deformation reflects that the inferred residual stress field is precise compared with the real residual stress within the annular part. The result indicates that the proposed layout optimization method for deformation force monitoring in annular parts is capable of achieving accuracy in inferring the residual stress field based on the deformation force.

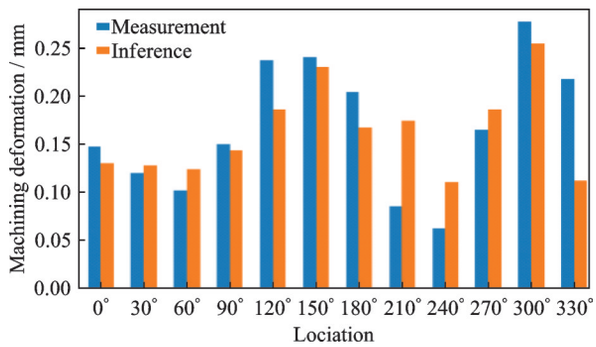

Fig.14 Machining deformation results

4 Conclusions

The proposed hierarchical optimization method is adaptable to varying settings, including geometries, materials and boundary conditions as long as the monitoring layout is optimized to ensure both the optimal equivalence of deformation force to residual force and inference ill-conditioning. Corresponding adjustments can be implemented in the FEM solution model and conveniently integrated to the proposed framework.

Despite its efficiency and effectiveness, the hierarchical optimization approach may encounter the difficulties in identifying globally optimal solutions. In future work, alternative multi-objective optimization methods incorporating learning-based method will be investigated to enhance the convergence speed. Moreover, cases with other materials such as titanium alloys will be explored to consider the impact of cutting-induced stress, expanding the applicability of the proposed layout optimization method.

References

[1] ZHANG Chenhong, YU Jianhua, ZHOU Lifeng, et al. Optimization analysis of clamping layout for thin-walled annular parts of aircraft engines[J]. Manufacturing Technology and Machine Tools, 2021(1): 21-24. (in Chinese)

[2] PONRAM R A, PRASAD B H, KUMAR S S. Thickness mapping of rocket motor casing using ultrasonic thickness gauge[J]. Materials Today: Proceedings, 2018, 5(5): 11371-11375.

[3] WU Q, WU J, ZHANG Y D, et al. Analysis and homogenization of residual stress in aerospace ring rolling process of 2219 aluminum alloy using thermal stress relief method[J]. International Journal of Mechanical Sciences, 2019, 157: 111-118.

[4] CHEN Junsong, LIU Changqing, ZHAO Zhiwei, et al. Inference method for residual stress field of titanium alloy parts based on latent Gaussian process introducing theoretical prior[J]. Transactions of Nanjing University of Aeronautics and Astronautics, 2024, 41(2): 135-146.

[5] ZHANG Hua, ZHAO Shengqiang, SUN Hao, et al. Investigation on the initial residual stress detection method and its application for deformation analysis in machining thin-walled blades[J]. Transactions of Nanjing University of Aeronautics and Astronautics, 2024, 41(2): 158-173.

[6] MA Y L, XUE N P, WU Q, et al. Residual stress analysis of a 2219 aluminum alloy ring using the indentation strain-gauge method[J]. Metals, 2020, 10(7): 979.

[7] LV N, LIU D, HU Y, et al. Research on the evolution of residual stresses in the manufacturing process of TC4 alloy profile rolled ring[J]. Engineering Failure Analysis, 2022, 137: 106269.

[8] LI Y, GAN W N, ZHOU W B, et al. Review on residual stress and its effects on manufacturing of aluminium alloy structural panels with typical multi-processes[J]. Chinese Journal of Aeronautics, 2023, 36(5): 96-124.

[9] GAO H J, ZHANG Y D, WU Q, et al. Investigation on influences of initial residual stress on thin-walled part machining deformation based on a semi-analytical model[J]. Journal of Materials Processing Technology, 2018, 262: 437-448.

[10] ZHU Y M, MAO K M, YU X X. A general model for prediction of deformation from initial residual stress[J]. The International Journal of Advanced Manufacturing Technology, 2020, 109(3): 1093-1101.

[11] TABATABAEIAN A, GHASEMI A R, SHOKRIEH M M, et al. Residual stress in engineering materials: A review[J]. Advanced Engineering Materials, 2022, 24(3): 2100786.

[12] SCHAJER G S, PRIME M B, WITHERS P J. Why is it so challenging to measure residual stresses?[J]. Experimental Mechanics, 2022, 62(9): 1521-1530.

[13] KHOSHAIM A B, ELSHEIKH A H, MOUSTAFA E B, et al. Prediction of residual stresses in turning of pure iron using artificial intelligence-based methods[J]. Journal of Materials Research and Technology, 2021, 11: 2181-2194.

[14] WANG S G, LI Y G, LIU C Q, et al. An initial residual stress inference method by incorporating monitoring data and mechanism model[J]. Chinese Journal of Mechanical Engineering, 2022, 35(1): 82.

[15] CHENG M H, JIAO L, YAN P, et al. Prediction of surface residual stress in end milling with Gaussian process regression[J]. Measurement, 2021, 178: 109333.

[16] ZHOU J H, ZHANG Z D, LIU C J, et al. Empirical modeling of residual stress profile for multi-axis milling GH4169G[J]. The International Journal of Advanced Manufacturing Technology, 2025, 137(3): 1405-1420.

[17] RISSAKI D K, BENARDOS P G, VOSNIAKOS G C, et al. Residual stress prediction of arc welded austenitic pipes with artificial neural network ensemble using experimental data[J]. International Journal of Pressure Vessels and Piping, 2023, 204: 104954.

[18] MIAO Z Y, MARGETTS L, VASILEIOU A N, et al. Surrogate model development using simulation data to predict weld residual stress: A case study based on the NeT-TG1 benchmark[J]. International Journal of Pressure Vessels and Piping, 2023, 206: 105014.

[19] FARIAS A, PASCHOALINOTO N W, BORDINASSI E C, et al. Predictive modelling of residual stress in turning of hard materials using radial basis function network enhanced with principal component analysis[J]. Engineering Science and Technology, an International Journal, 2024, 55: 101743.

[20] LI B T, ZHU J J, ZHAO X F, et al. Residual stress prediction in laser shock peening induced LD-TC4 alloy by data-driven ensemble learning methods[J]. Optics & Laser Technology, 2024, 176: 110946.

[21] PRADHAN R, ALTALBAWY F M A, KHAN A R, et al. A FEM-guided data-driven machine learning model for residual stress characterization in ultrasonic surface rolling of lightweight alloys[J]. Applied Physics A, 2024, 130(6): 400.

[22] ZHAO Z W, LIU C Q, LI Y G, et al. A new method for inferencing and representing a workpiece residual stress field using monitored deformation force data[J]. Engineering, 2023, 22: 49-59.

[23] ALGREDO-BADILLO I, CONDE-MONES J J, HERNÁNDEZ-GRACIDAS C A, et al. An FPGA-based analysis of trade-offs in the presence of ill-conditioning and different precision levels in computations[J]. PLoS One, 2020, 15(6): e0234293.

[24] GUI Qingming, GUO Jianfeng, BIAN Shaofeng. Ill-conditioning diagnostics based on eigensystem[J]. Developments in Surveying and Mapping, 2002, 27(2): 13-15, 19. (in Chinese)

[25] LI Z C, HUANG H T, WEI Y M. Ill-conditioning of the truncated singular value decomposition, Tikhonov regularization and their applications to numerical partial differential equations[J]. Numerical Linear Alge-

bra with Applications, 2011, 18(2): 205-221.
[26] REICHEL L, RODRIGUEZ G. Old and new parameter choice rules for discrete ill-posed problems[J]. Numerical Algorithms, 2013, 63(1): 65-87.
[27] DEWAELE N, VANNIEUWENHOVEN N. Which constraints of a numerical problem cause ill-conditioning?[J]. Numerische Mathematik, 2024, 156(4): 1427-1453.
[28] SU Honghua, WANG Yufeng, QIAO Mu, et al. Review current questions and strategies about finite element simulation for cutting processing[J]. Jounal of Nanjing University of Aeronautics and Astronautics, 2023, 55(3): 361-378. (in Chinese)
[29] ZHU Qian, ZHAO Junhai, ZHANG Changguang, et al. Elastic-brittle-plastic unified solutions of limit internal pressure for double-layered combined thick-walled cylinder[J]. Engineering Mechanics, 2015, 32(9): 68-75. (in Chinese)
[30] ZHAO Z W, LI Y G, LIU C Q, et al. Predicting part deformation based on deformation force data using Physics-informed Latent Variable Model[J]. Robotics and Computer-Integrated Manufacturing, 2021, 72: 102204.

Acknowledgements This work was supported in part by the General Program of the National Natural Science Foundation of China (No.52175467) and the National Key R&D Program of China (No.2022YFB3402600).

Authors

The first author Mr. **DAI Kaining** received his B.S. degree in mechanical engineering from Shanghai Jiaotong University, Shanghai, China, in 2020. He is currently pursuing his M.S. degree in Nanjing University of Aeronautics and Astronautics, Nanjing, China. His research interests are machining deformation prediction and control.

The corresponding author Prof. **LI Yingguang** received his B.S. and Ph.D. degrees from Nanjing University of Aeronautics and Astronautics, Nanjing, China, in 1999 and 2004, respectively. He has worked as professor with Nanjing University of Aeronautics and Astronautics since 2008. His research interests are focused on data-driven intelligent manufacturing and advanced composite curing technology.

Author contributions Mr. **DAI Kaining** designed the study, conducted the simulation and analysis, interpreted the results and wrote the manuscript. Prof. **LIU Changqing** optimized the overall idea and feasibility of the proposed method. Mr. **WANG Enning** conducted the experiments and processed the data. Dr. **ZHAO Zhiwei** contributed to improvement of the method details. Prof. **SALONITIS Konstantino** contributed to the review and structure refinement of thesis. Prof. **LI Yingguang** guided on the research and manuscript improvement. All authors commented on the manuscript draft and approved the submission.

Competing interests The authors declare no competing interests.

(Production Editor: ZHANG Bei)

环形件变形力监测布局的层次优化方法

代凯宁[1]，刘长青[1]，王恩宁[1]，赵智伟[1]，SALONITIS Konstantino[2]，李迎光[1]

(1.南京航空航天大学机电学院，南京 210016，中国；
2.克兰菲尔德大学可持续制造系统中心，克兰菲尔德 MK43 0AL，英国)

摘要：获取残余应力对于控制环形件的加工变形至关重要，直接影响关键部件在高端装备中的性能与稳定性。尽管现有研究在加工过程中对变形力进行监测，通过基于变形力的方法实现了零件的全局残余应力场推断，但在复杂的加工条件下，可靠的变形力数据获取仍面临较大挑战。本文提出了一种面向环形件的变形力监测布局层次优化方法。该方法基于对环形件中变形力与残余应力之间关系的分析建立了等效性与病态性两个优化目标。该方法通过局部变形评估变形力与残余应力在导致加工变形方面的效果等效性，并进一步对通过变形力推断残余应力场的病态性进行优化，以提升推断过程的稳定性。本文在仿真环境和实际加工实验中对所提出的布局优化方法进行了验证，验证结果表明该方法能够有效提升基于变形力推断环形件残余应力场的精度。

关键词：残余应力；环形件；变形力；布局优化